1987 IEEE Int'l Conf. Robotics and Automation

Some Experiments with Tactile Sensing during Grasping

R.S. Fearing

Stanford Artificial Intelligence Laboratory
Department of Computer Science, Stanford, CA 94305

ABSTRACT

A tactile sensing finger tip for the Stanford/JPL Hand has been developed. This sensor incorporates an 8×8 sensor array with complete coverage of the cylindrical finger tip. A preliminary analysis has been done to determine contact center, magnitude, and orientation, and to judge if the constructed sensor has adequate sensitivity and density. This low level tactile information provides the first steps needed for reliable object manipulation in a dextrous hand. Experiments were performed during an open loop re-grasping manipulation to determine how well the sensors and algorithms performed.

1. Introduction

Local contact information from the fingers is important for dextrous manipulation with multifingered hands. Some of the most useful parameters to recover are angle and magnitude of force, surface normals, location of contact, and type of contact (point, line, plane) see for example, [Fearing, 1984]. The location of the contact on the finger is necessary for accurate force application. Two different approaches to obtaining contact information are a finger tip sensor that gives location and resultant force using a strain gauge structure [Brock and Chiu, 1985], and arrays of deflection transducers [Hillis 1981, Boie 1984, Chun and Wise 1985, and Siegel et al 1985]. The finger tip array sensor approach has an advantage for simultaneously resolving multiple contacts, which are common in multifinger grasping.

A tactile sensor array was packaged in a finger tip and mounted on the Stanford/JPL hand (Fig. 1). There are 7×8 tactile elements (tactels) on the cylindrical portion, and 1×8 elements under the hemispherical tip. This low density is sufficient for initial experimentation, but it could be easily expanded. This finger is a prototype device for sensory and manipulation research. Other cylindrical finger tips are a 133 element device described in [Allen and Bajczy, 1985] and a 256 element fiber-optic device [Begej, 1986].

This paper describes steps taken towards "closing the loop" between finger tactile sensor input and finger force output. The grasping and sensor implementations are described, and a sensor interpretation scheme based on interpolation is developed. The contact information from a manipulation is analysed off line to track the object center.

2. Grasping Implementation

The Stanford/JPL hand [Salisbury and Craig, 1982] uses force control in spherical coordinates to manipulate objects. The implementation of an object reorientation strategy called

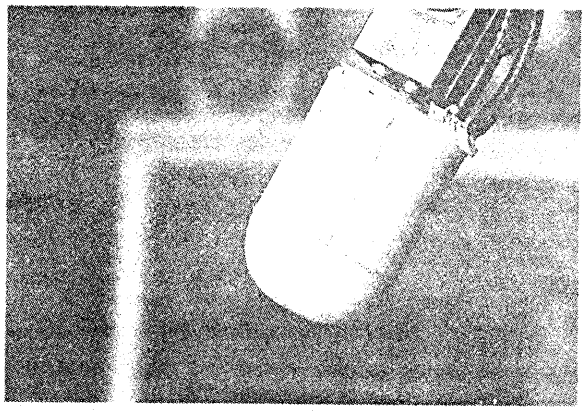

Figure 1. Tactile sensing finger mounted on Stanford/JPL hand.

"twirling" is described in [Fearing, 1986]. In twirling, an object is successively grasped and regrasped by succeeding pairs of fingers to cause large rotations of the object with respect to the hand. Twirling is one of 3 basis rotations that can be combined to arbitrarily reorient a grasped object.

The force control system for the fingers uses a tendon tension servo running at a high rate to control tendon tensions and joint torques, and a slower servo using the joint jacobian to calculate desired joint torques from desired forces in spherical coordinates. The desired forces are pre-calculated to control object behavior, so the manipulation of the object is in essence open loop. The system of forces is chosen so that object slip at the fingers is bounded, and the object remains quasi-statically stably grasped.

The finger control system first ran on a PDP 11/60 as described in [Fearing, 1986], and now runs on the NYMPH multiprocessor system [Chen, et al 1986a, 1986b]. Fig. 2 shows the processor arrangement used. Two 10 MHz National 32016 processors are used for the tension servo (running at 480 Hz) and force servo (at 120 Hz) for each finger. A seventh coordination processor sends desired finger force and location commands to each finger. A bar can be reoriented in the twirl operation at about 2 revolutions (720°) per minute. Due to unmodelled effects such as gravity, varying contact friction forces, and friction in the hand mechanism, the object may only "twirl" for about two revolutions before it is dropped. There is also a dedicated processor for each finger to be used for tactile processing. This paper describes some preliminary tactile information interpretation during grasping, but the tactile information is not yet used in the control loop to correct finger forces and directions.

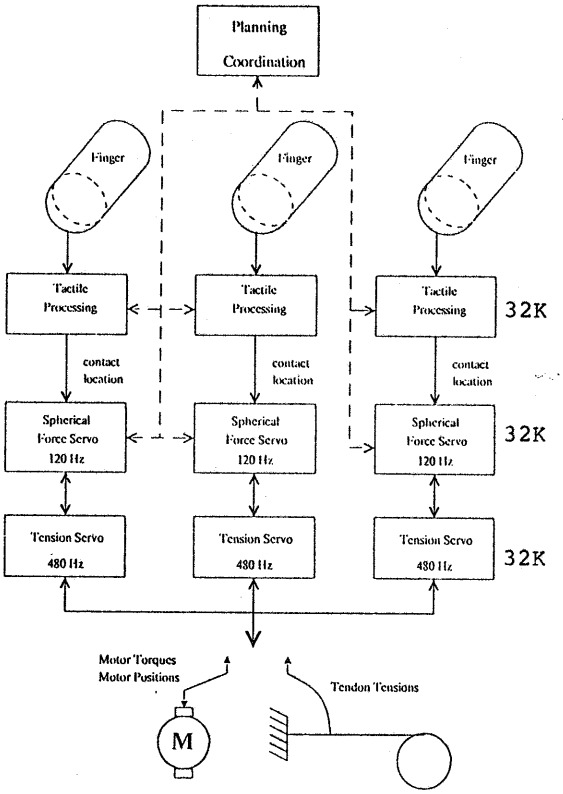

Figure 2. Multiprocessor control system for Stanford/JPL hand.

3. Sensor Implementation

Fig. 3 shows the finger tip sensor, which uses an array of capacitors formed at the junctions of perpendicular conductive strips. The lower plates of the capacitor are 8 "stripes" of copper spaced at 45° around the cylinder axis. The upper plates are 7 "rings" of copper spaced at 3.7 mm along the length of the cylinder. An annulus at the tip gives coverage under the hemisphere. The capacitors are covered with a 3.8mm thick skin of rubber to reduce spatial aliasing [Fearing and Hollerbach, 1985]. More complete details of the finger construction are in [Fearing et al, 1986]

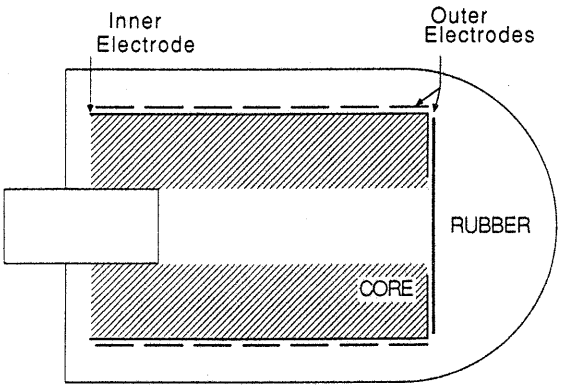

Figure 3. Finger tip construction.

Standard capacitive sensing techniques [Siegel et al, 1986; Boie 1984] are used. An amplitude measurement scheme gives a voltage output proportional to the sensor capacitance. The sensor is scanned at a 15 Hz rate, which is adequate for initial work, but can be increased. The electronics are mounted remotely at the base of finger for ease of fabrication and to separate the electrical and mechanical design considerations.

To approximate measuring the subsurface strain normal to the surface ϵ_z with capacitor plate separation d_o and deflection Δd, we use:

$$\frac{\Delta d}{d_o} \approx \epsilon_z \tag{2}$$

for d_o small, and $\Delta d \ll d_o$. Assuming that the capacitors can be approximated as parallel plate capacitors, and ignoring tilting of plates (parallel translation of the plates has no effect), the percent deflection signal is obtained by:

$$\frac{V_S - V_o}{V_S} = 1 - \frac{C_{So}}{C_S} = 1 - \frac{\frac{1}{d_o}}{\frac{1}{d_o - \Delta d}} = \frac{\Delta d}{d_o}, \tag{3}$$

where V_S is the sensed voltage from a capacitive element, V_o is the voltage with no deflection, and C_{So}, C_S are the nominal and deflected capacitance values. This ratio of voltage measurements is a well behaved function.

4. Sensory Interpretation

Because the sensor has spatial low pass properties due to the thickness of the elastic medium, a continuous deflection signal can be reconstructed from the discrete percent deflection samples if the applied pressure distribution is bandlimited. Because of the low sensor density, good localization requires sub-tactel interpolation of contact features. Some work has been done on identifying and locating objects given the contact locations [Gaston and Lozano-Perez, 1983; Shekhar et al 1986]. The problem addressed here is how to find the contact locations with a low density sensor.

The spatially sampled tactile response is converted into a continuous function for analysis. Let z_{ij} be an 8×8 array formed from the percent deflection of all tactels ij. The interpolated deflection function is:

$$f(x,y) = \tag{4}$$
$$\sum_{i=0}^{N-1} \sum_{j=0}^{N-1} z_{ij} \frac{\sin\pi(x-i)\sin\pi(y-j)}{\pi^2(x-i)(y-j)} w(x-i)\, w(y-j).$$

Here x, y are in tactel spacing units, where distances are normalized by dividing by the sensor spacing b. Note that because the sensors are on a cylinder, z_{0j} and z_{7j} are adjacent, so boundary problems are avoided along that axis. The 8 tip elements $z_{00} \cdots z_{07}$ are included in the expression, although they should be treated as a special case. $w()$ is the Hanning window [Oppenheim and Schafer, 1975] which is

$$w(n) = \begin{cases} \frac{1}{2}[1 - \cos(\frac{2\pi n}{N-1})], \text{ for } 0 \le n \le N-1 \\ \text{and 0 otherwise} \end{cases} \tag{5}$$

and N is the total number of samples. The window makes the low pass filter finite in extent, and reduces ringing. The sinc interpolation function has lower resolution and interpolation errors than other common interpolation filters such as Gaussians and Cubic B-splines [Pratt, 1978].

4.1. Localization

For certain contact types with small or symmetric convex objects, the maximum pressure point corresponds to the center of the object. The impulse response for a normal force using the plane stress assumption is [Fearing et al, 1986]:

$$h(y) = \frac{-2d}{\pi E r^4}[d^2 - \nu y^2]. \tag{6}$$

where E, d, ν are the modulus of elasticity, the sensor depth, and Poisson's ratio respectively, and r is the distance from the force on the surface to the sensor. This is an even function with a maximum at the origin. The subsurface strain is found by convolution of the impulse response with the applied pressure $p(y)$ (see [Fearing and Hollerbach, 1985] for more details):

$$\epsilon_x(y) = \int_{y_o=-\infty}^{\infty} p(y-y_o)h(d, y_o)dy_o \tag{7}$$

If an even pressure is applied on the surface with a maximum at the origin, the location of the maximum normal strain will correspond to the location of the center of pressure. A similar argument can be made for the three dimensional case.

To find the maximum deflection and its location for an unknown pressure, iterative techniques are used. The conditions for a maximum of a surface are:

$$\frac{\partial f}{\partial x} = 0, \frac{\partial f}{\partial y} = 0, \frac{\partial^2 f}{\partial x^2} < 0, \text{ and } \frac{\partial^2 f}{\partial y^2} < 0. \tag{8}$$

Using Newton-Raphson (Thomas, 1968) to find where the slopes are zero, we have the updated position

$$\begin{bmatrix}\Delta x \\ \Delta y\end{bmatrix} = -\begin{bmatrix}\frac{\partial^2 f}{\partial x^2} & \frac{\partial^2 f}{\partial x \partial y} \\ \frac{\partial^2 f}{\partial y \partial x} & \frac{\partial^2 f}{\partial y^2}\end{bmatrix}^{-1}\begin{bmatrix}\frac{\partial f}{\partial x} \\ \frac{\partial f}{\partial y}\end{bmatrix}. \tag{9}$$

Convergence to 0.01 tactel starting from the maximum z_{ij} tactel is observed in typically two or three steps. Fig. 4 shows recovery of the probe location along the central portion of the cylinder length. A 50 gm load on a 3 mm diameter spherical tip probe is centered above a stripe, and the probe is moved at 250 μm increments along the stripe. The ripple on the peak deflection location is mainly due to aliasing. Aliasing is less severe than predicted by the simple plane stress model with a line load, (see [Fearing, et al 1986]), so position of the probe is within ± 12 % of ideal, for a positioning error of ± 0.5mm. Note that the aliasing error is zero when the probe is directly above a tactel, because the sinc interpolation passes through the sample points.

Localization performance around the circumference of the finger was done in the same manner, by applying the probe at 3° increments. The localization error is larger, about ± 10° (Fig. 5). This is about ±2.3 mm error along the circumference.

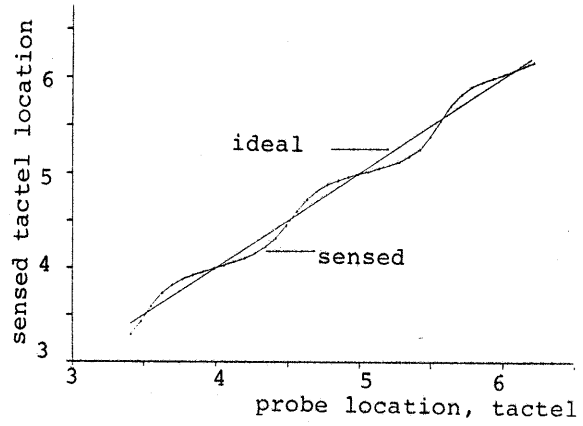

Figure 4. Localization errors along finger length.

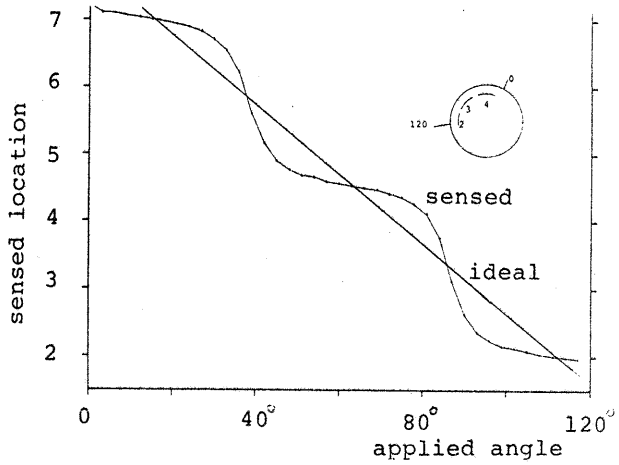

Figure 5. Localization errors around finger circumference.

4.2. Force Recovery

The use of the continuous deflection function $f(x, y)$ to recover total normal load and the angle of force for some contacts was described in [Fearing et al 1986] for the two dimensional case. For contact areas large compared to the sensor depth, the contact pressure can be approximated as zero frequency, so

$$F_x \approx 2E \int_{y=-\infty}^{\infty} \epsilon_x(y)dy \tag{10}$$

where F_x is the total force in the normal direction per unit length Nm^{-1}, and $\epsilon_x(y)$ is recovered by interpolation.

To recover the angle of force from just the normal deflection when the contact pressure is even, the interpolated deflection function is split into even and and odd components. The ratio of maximum odd to maximum even deflection gives the relative force angle. This was demonstrated in [Fearing et al 1986].

4.3. Contours

A useful tool for analyzing the sensor output is a plot of equal percent deflection contours. The conditions for equal deflection contours of height k are:

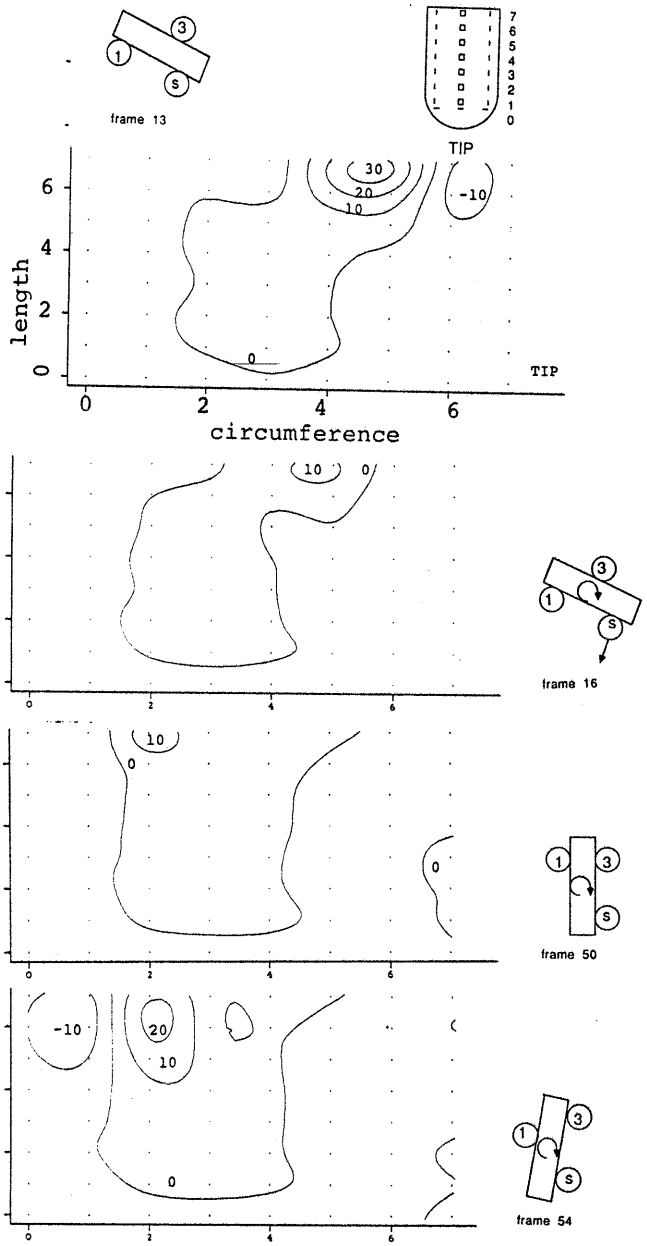

$$f(x,y) = k, \frac{\partial f}{\partial x} = f_x = 0, \frac{\partial f}{\partial y} = f_y = 0. \quad (11)$$

The direction of constant height on the surface is given by

$$\phi = -\tan^{-1}\frac{f_x}{f_y} \quad (12)$$

The contours are found iteratively from the position update vector

$$\Delta\underline{x} = \begin{bmatrix}\Delta r\cos\phi \\ \Delta r\sin\phi\end{bmatrix}, \quad (13)$$

where Δr is the step size. The height error at the new location, $f(\underline{x}+\Delta\underline{x}) - k$, is used to adjust the new x and y locations to insure staying on the contour. The low pass characteristic insures that the deflection surface is well behaved. Contour plots are used in the next sections as a graphic tool for identifying sensor behavior and contact shape.

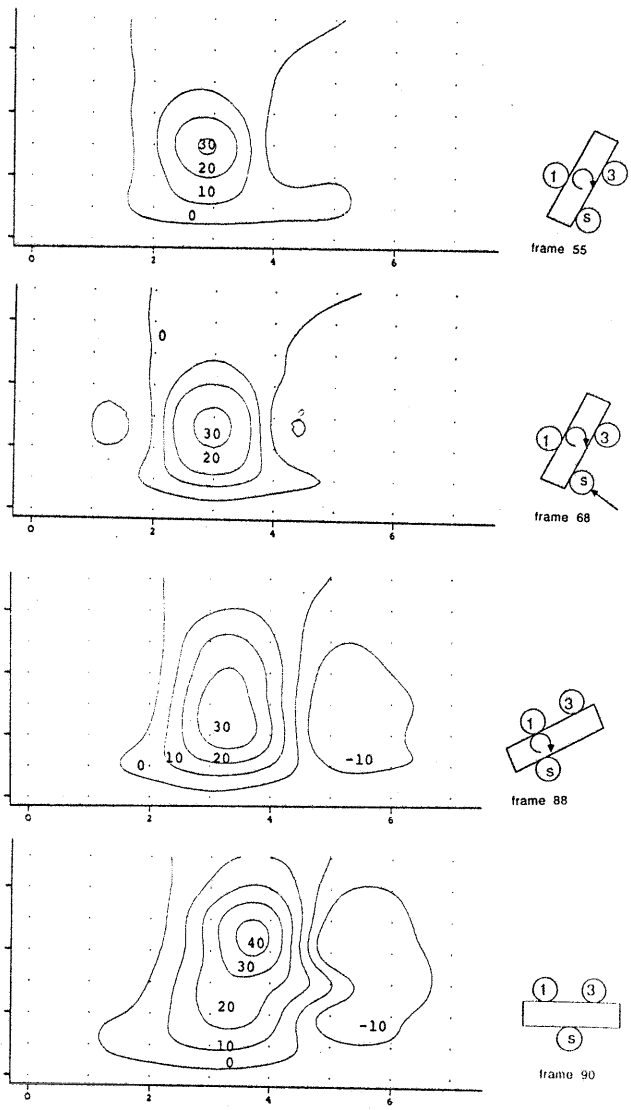

Figure 6. Iso-deflection contours on sensor during twirl.

5. Contact Localization During Grasping

The tactile sensor array was recorded during a twirling operation of a small bar. 100 frames of tactile information were saved at 6 Hz. This rate gives about 10 tactile frames for each grasping operation. These operations are commands given to the finger to apply force directed to another finger, roll about a finger, fix the finger in space, and remove the finger from contact.

Fig. 6 shows contour plots of the tactile data taken from the sensor mounted on finger 2 (F2) for the more interesting frames. In the contour plots, the tip of the sensor is at the bottom of the plot, row 0, and the horizontal axis corresponds to the circumference of the cylinder.

The sequence begins with the object grasped with all three fingers, and the grasp is being changed to just finger 1 (F1) and finger 3 (F3). The force at F2 is reduced, and F2 is removed from contact with the object at frame 17. F2 is

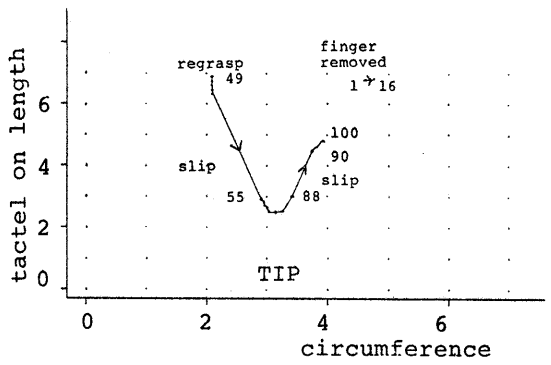

Figure 7. Center of pressure on finger during twirl operation.

moved in space around the object to the other side, and contact does not occur until frame 50. Note that the contact location is now about 90° from where it was previously. As the force at F2 increases, the object rolls as seen in frame 54.

The twirl strategy only controls the forces in the finger plane, and neglects the orientation of the last joint of the finger. Between frame 54 and frame 55, the object twisted in the hand, so it was skewed with respect to the twirling plane. The object also slipped along the length of the finger when the force was increased at F2. In frame 68, the force at F3 is being reduced in preparation for F3 to move to the other side of the object. In frame 88, F1 and F3 are now on the opposite side of the object from the sensing finger, so the applied force increases to its maximum value as expected (frame 90).

The center of pressure for all 100 frames that had contact was tracked and is shown in Fig. 7. Frames 1 to 16 show rolling of the object about the sensor. Slip is indicated by large contact displacements in very short time, and seems most likely to occur when the grasp changes from 2 to 3 fingers. Because of uncertainty in finger position, the force control system is not able to apply forces in exactly the right direction. Slip is expected and tolerated around the circumference of the finger, but is not desirable along the length of the finger for twirling.

6. Line Orientation on Cylinder

The previous section demonstrated how an object can have undesired rotations during grasping. For good grasping control, the orientation of the object in the fingers should be known. This section considers determining the orientation of an object on the finger when the object has a significantly smaller radius than the finger, and can be approximated as a line load on a cylinder.

The problem of determining the orientation of a line contact on a flat tactile sensor array has been considered previously by Driels [1986] and Shekhar et al [1986]. Driels used moments to get line orientation within about ± 2.5° using a 16×16 array. Shekhar et al considered using the least square fit of an edge.

Determining the orientation of a line on a cylindrical sensor array is harder than for a flat array. Even with large deformations, only about 90° of the cylinder's sensors will have a force above them. In addition, both the contact area and contact length change with orientation of the line on the finger. It is important to have a soft sensor, or the contact will be a small, indistinguishable ellipse except when the line and the

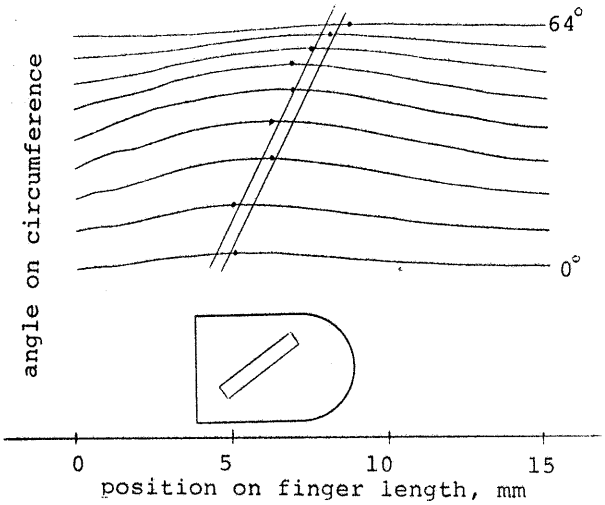

Figure 8. Deflection pattern for virtual 9×25 sensor.

sensor axis are aligned. As in vision, a rectangular array has angle dependent quantization effects [Gordon and Seering, 1986].

To show in principle that it is possible to determine line orientation with this finger diameter, skin softness, and sensor depth, a higher density "virtual" tactile sensing scheme was used. If the sensor is spatially invariant about the cylindrical portion, higher equivalent density can be had by multiple measurements of one tactel as the object is scanned about the finger. Fig. 8 shows 9×25 measurements of a 4.8 mm radius rod at 30° from the longitudinal axis with a 200 gm load. The equivalent sensor spacing is 0.635mm × 8.0°. The dots indicate the peak deflection for each measurement along the finger axis. The orientation is observable in the figure, but is somewhat obscured by the low pass filtering at the sensor depth and the short contact length.

Fig. 9 shows the approximation used for a line on a cylinder, which will be used to determine orientation with just one set of measurements. The width of the contact is given by

$$w = 2\sqrt{\delta\,(2r_f - \delta)} \tag{11}$$

where $r_f \approx$ 12.7 mm is the finger radius. Experimentally, for a 2 N load on a 4.4 mm rod perpendicular to the sensor cylinder, the orientation angle $\gamma = 0$, the cylinder deformation $\delta \approx$ 0.6mm. So using eq. (11) the maximum width is just $w_{\max} \approx$ 7.5 mm. In angle, this is about 34° around the circumference, which is less than the angular sensor spacing. For larger angles, the contact length will be longer, and w will be shorter, because of the reduced pressure per unit length on the line for the same total load.

Given the ends of the indenting cylinder where it leaves contact with the finger (at location z_e), the angle γ can be determined from

$$\gamma = \tan^{-1}\frac{2z_e}{w}. \tag{12}$$

Using the measured localization errors $\Delta z_e \approx$0.5 mm and $\frac{\Delta w}{2} \approx$ 2.3 mm from Section 4.1, a crude estimate of orientation sensing capability is obtained from:

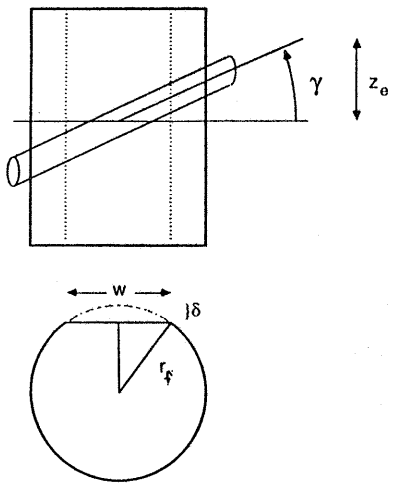

Figure 9. Model of line contact on cylinder.

$$\Delta\gamma = \frac{\partial\gamma}{\partial z_e}\Delta z_e + \frac{\partial\gamma}{\partial w}\Delta w, \tag{13}$$

or

$$\Delta\gamma = \frac{1}{2}\frac{w\,\Delta z_e - z_e\,\Delta w}{(\frac{w}{2})^2 + z_e{}^2}. \tag{14}$$

For a contact at 45°, the worst case error could be up to +22°. The main contributor to the large orientation uncertainty is the poor localization performance around the circumference. The localization about the circumference could be improved by using anti-aliasing techniques.

The problem is to find z_e and w from the percent deflection profile. For line contact not parallel to finger axis, it will be assumed that the contact pressure will be symmetric about the ends of the line and zero at the ends. The strain impulse response of the elastic medium will preserve the pressure symmetry. To find the angle γ it is not necessary to find the ends of the contact between the line and the finger, but only two points beneath the line, forming a line parallel to the applied line.

Because of the low pass elastic medium, finite line contacts will tend to elliptical iso-deflection contours in $f(w, z)$. If the deflection is approximated as an ellipse, the major axis of the ellipse will correspond to to the indenting line's axis, if the line contact length is greater than the impulse response width. One problem with this ellipse is that there is a 90° ambiguity when the contact length is small (the pressure is low), and the ellipse becomes circular. This typically occurs around 45°.

A preliminary algorithm for orientation uses the maximum spanning line of the isodeflection contour at 75% of peak deflection. This line corresponds to the major axis of the ellipse. Experiments were conducted with a 4.7 mm radius rod applied with 2 N force. Fig. 10 shows contour plots for contacts at 20° and 70° with the maximum spanning lines marked. Fig. 11 shows measured orientation angle as the 4.7 mm radius cylinder is rotated from $\gamma = 0°$ to 90°. The measured orientation error is worst (almost 20° error) at 50°. This is not too bad for in effect only 2×7 sensors along the cylinder.

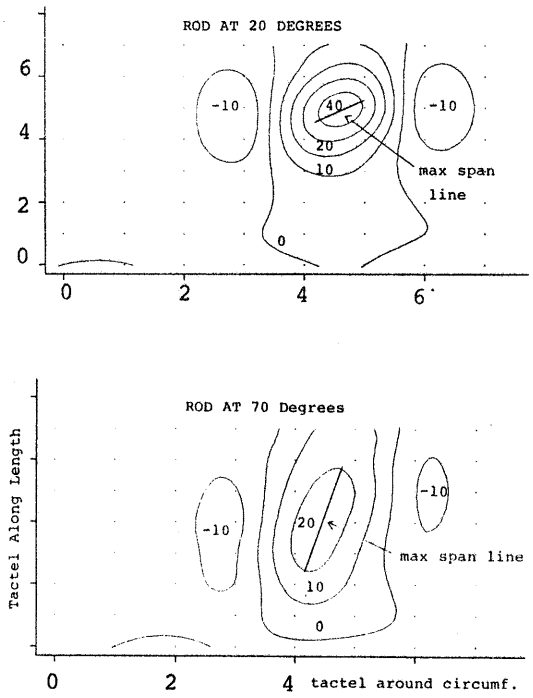

Figure 10. Iso-deflection contours for 20° and 70° orientation.

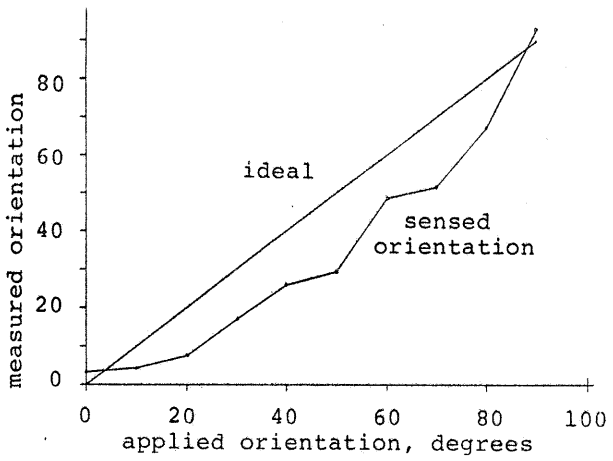

Figure 11. Orientation using maximum spanning line of iso-deflection contour.

For wider contacts, there will be more orientation ambiguity. If the deflection contours have two axes of symmetry, the object could be determined to one of two possible orientations. One would need *a priori* knowledge to decide which is correct. If the deflection were directly available, simple methods for determining object curvature like those described in [Gurfinkel et al 1974] could be used.

Discussion

Sub-tactel localization has been demonstrated in tracking the center of pressure, but it is not good enough to determine the line orientation very well using the preliminary methods described here. An orientation error of 20° is not sufficient for very accurate manipulation. However, with three finger sensors the error may be reduced to only 7° by combining them. This may indicate a requirement for higher sensor density around the cylinder. This could be had by moving sensors to the more central grasp area, flattening out the cylinder to increase contact area, or going to 8×16 sensors. A thicker skin is probably not indicated, because it will make the iso-deflection ellipses more circular, although a softer skin might be desirable to increase contact size.

Acknowledgment

This work was supported by DARPA contract MDA903-86-K-0002. Many thanks to A. Rise and G. Gorali for their knowledge and assistance, to V. Nalwa, G. Healey, S. Shekhar, B. Armstrong, and D. Kriegman for helpful dialogue, and to T. Binford for his continuing encouragement and insights.

REFERENCES

[1] P. Allen and R. Bajczy, "Object Recognition using Vision and Touch," 9th Intern. Joint Conf. on Artificial Intelligence, Los Angeles, August, 1985.

[2] Begej Corporation, "Model FTS-2 Fingertip-shaped Tactile Sensor," Technical Bulletin #2, October 1986.

[3] R. A. Boie, "Capacitive Impedance Readout Tactile Image Sensor," IEEE Intern. Conf. on Robotics and Automation, Atlanta, GA, March, 1984.

[4] D. Brock and S. Chiu, "Environment Perception of an Articulated Robot Hand Using Contact Sensors," ASME Winter Annual Meeting, Miami, FL, 1985.

[5] J.B. Chen, R.S. Fearing, B.S. Armstrong, and J.W. Burdick, "NYMPH: A Multiprocessor for Manipulation Applications", IEEE Intern. Conf. on Robotics and Automation, San Francisco, CA April, 1986.

[6] J.B. Chen, B.S. Armstrong, R.S. Fearing, J.W. Burdick, "Satyr and the Nymph: Software Archetype for Real Time Robotics," IEEE-ACM Joint Computer Conference, Dallas, November 1986.

[7] K. Chun and K.D. Wise, "A High Performance Silicon Tactile Imager Based on a Capacitive Cell," *IEEE Trans. on Elect. Devices*, vol. ed-32, no. 7, July 1985.

[8] M.R. Driels, "Pose Estimation using Tactile Sensor Data for Assembly Operations," IEEE Intern. Conf. on Robotics and Automation, San Francisco, CA April, 1986.

[9] R.S. Fearing, "Simplified Grasping and Manipulation with Dextrous Robot Hands", American Control Conference, San Diego, CA, June 1984.

[10] R.S. Fearing and J.M. Hollerbach, "Basic Solid Mechanics for Tactile Sensing," *Intern. Jnl. of Robotics Research*, vol. 4, no. 3, Fall 1985.

[11] R.S. Fearing, "Implementing a Force Strategy for Object Re-orientation," IEEE Intern. Conf. on Robotics and Automation, San Francisco, CA April, 1986.

[12] R.S. Fearing, A. Rise, and T.O. Binford, "A Tactile Sensing Finger Tip for a Dextrous Hand," SPIE Conference on Intelligent Robotics and Computer Vision, Cambridge, MA October 1986.

[13] S. J. Gordon and W.P. Seering, "Accuracy Issues in Measuring Quantized Images of Straight-Line Features," IEEE Intern. Conf. on Robotics and Automation, San Francisco, CA April, 1986.

[14] P.C. Gaston and T. Lozano-Perez, "Tactile recognition and localization using object models: the case of polyhedra on a plane," M.I.T. A.I. Memo, March, 1983.

[15] V.S. Gurfinkel, A. Yu. Shneyder, Ye. M. Kanayev, and Ye. V. Gurfinkel, "Tactile Sensitizing of Manipulators", *Engineering Cybernetics*, Vol. 12, No. 6, Nov. 1974.

[16] Hillis, W.D. "Active touch sensing," S.M. thesis, M.I.T. Department of Electrical Engineering and Computer Science 1981.

[17] Oppenheim, A.V. and Schafer, R.W. *Digital Signal Processing*, Englewood Cliffs: Prentice-Hall 1975.

[18] W.K. Pratt, *Digital Image Processing*, John Wiley & Sons, 1978.

[19] J.K. Salisbury and J.J. Craig, "Articulated Hands: Force Control and Kinematic Issues," *International Journal of Robotics Research*, Vol. 1, No. 1, Spring 1982.

[20] S. Shekhar, O. Khatib, M. Shimojo, "Sensor Fusion and Object Localization," IEEE Intern. Conf. on Robotics and Automation, San Francisco, CA April, 1986.

[21] D.M. Siegel, I. Garabieta, J.M. Hollerbach, " A Capacitive Based Tactile Sensor," SPIE Conf. on Intelligent Robots and Computer Vision, Cambridge, MA Sept. 1985.

[22] D.M. Siegel, "Contact Sensors for Dextrous Robotic Hands," MIT AI Lab Technical Report 900, June 1986.

[23] G.B. Thomas, *Calculus and Analytic Geometry* Reading, MA: Addison-Wesley 1968.